

Impact Toughness Analysis of a High Strength Steel Hardox 450 Welded Joint

Vagner Machado Costa¹ , Pedro Henrique Costa Pereira da Cunha² , Eduardo da Rosa Vieira³ 

¹ Instituto Federal de Educação, Ciência e Tecnologia Sul-riograndense – IFSul, Charqueadas, RS, Brasil.

² Instituto Federal de Educação, Ciência e Tecnologia do Rio Grande do Sul – IFRS, Caxias do Sul, RS, Brasil.

³ Instituto Federal de Educação, Ciência e Tecnologia do Rio Grande do Sul – IFRS, Rio Grande, RS, Brasil.

How to cite: Costa VM, Cunha PHCP, Vieira ER. Impact toughness analysis of a high strength steel hardox 450 welded joint. *Soldagem & Inspeção*. 2023;28:e2802. <https://doi.org/10.1590/0104-9224/SI28.02>

Abstract: This work aims to analyze the influence of low temperature on the toughness of a high-strength steel HARDOX 450° joints welded by the Metal Core Arc Welding (MCAW) process. Impact toughness tests (Charpy V-notch test) were performed on the 10 mm base metal (BM), weld metal (WM), and heat-affected-zone (HAZ) at temperatures of -100 °C, -80 °C, -60 °C, -20 °C, 0 °C, and 25 °C to obtain the ductile-brittle transition curve for each of these regions. Additionally, the tensile test and metallographic characterization were performed in order to complement the evaluation of the welded joint. The results of the impact tests showed higher toughness values of the base metal compared to the other two regions of the weld joint analyzed (WM and HAZ). The low toughness present in the HAZ is related to its microstructure composed of Widmanstätten ferrite and coarse grain. However, temperatures of -100 °C and -80 °C show the absorbed energy values in the three regions remarkably close to each other (between 11 J and 20 J).

Key-words: Charpy; Ductile-brittle; MCAW.

Análise da Tenacidade ao Impacto de uma Junta Soldada de um Aço de Alta Resistência Hardox 450

Resumo: O presente trabalho visa analisar a influência da temperatura baixa na tenacidade ao impacto de juntas de aço de alta resistência HARDOX 450° soldadas através do processo Metal Core Arc Welding (MCAW). Para tanto foram realizados ensaios de tenacidade ao impacto (ensaio de Charpy com entalhe em V) no metal base de 10 mm (MB), no metal de solda (MS) e na zona termicamente afetada (ZTA) nas temperaturas de -100 °C, -80 °C, -60 °C, -20 °C, 0 °C e 25 °C com o objetivo de levantar a curva de transição dúctil-frágil para cada uma dessas regiões. Adicionalmente, foi realizado ensaio de tração e caracterização metalográfica a fim de complementar a avaliação da junta soldada. Os resultados dos ensaios de impacto mostraram maiores valores de tenacidade do metal base em relação às outras duas regiões da junta soldada analisada (MS e ZTA). A baixa tenacidade apresentada na ZTA está relacionada à sua microestrutura composta por ferrita de Widmanstätten e grão grosseiro. Contudo, as temperaturas de -100 °C e -80 °C apresentam os valores de energia absorvida nas três regiões bem próximos entre si (de 11 J a 20 J).

Palavras-chave: Charpy; Dúctil-frágil; MCAW.

1. Introduction

Nowadays, industries are focused on the manufacture of components and equipment subject to excessive abrasion wear, mainly in the mining area (conveyors, crushers, gutter lining, among others), off-road trucks, road and agricultural implements [1], are continually working to improve the products developed. Thus, the engineering sector of companies progressively seeks high-performance metal alloys that meet their requirements. Therefore, a new generation of steels, categorized as low-alloy, quenched, and tempered abrasion-resistant steels or low-alloy martensitic steels, are being used extensively to meet this demand [2-5]. These steels have high hardness martensitic microstructure over the entire sheet thickness, due to the combination of carbon and alloying elements, such as Mn, Ni, Mo, Cr, and B, which are often added to structural steels to improve strength and toughness through modification of the microstructure [6]. Also, it is known that Boron is an effective agent to increase the hardenability of steels [4,7]. Therefore, it is possible to achieve high strength after the quenching process with the use of low cooling rates. High strength quenched and tempered steel is being widely used in applications where high levels of mechanical strength are required (it has a tensile strength higher than 1200 MPa) and abrasion resistance, combining toughness and weldability [8]. These steels have good weldability, and the arc welding processes are the most common technique used. Among these processes, the MCAW has been gaining more space due to the operational

Received: 16 June, 2021. Accepted: 20 Jan., 2023.

E-mails: vagnercosta@ifsul.edu.br (VMC), pedrohcnha@hotmail.com (PHCP), eduardo.vieira@riogrande.ifrs.edu.br (ERV)



This is an Open Access article distributed under the terms of the [Creative Commons Attribution license](https://creativecommons.org/licenses/by-nc/4.0/), which permits unrestricted use, distribution, and reproduction in any medium, provided the original work is properly cited.

characteristics, such as versatility, good productivity, high deposition rate. Besides, it has metallurgical benefits due to the internal flux in the weld metal deposited [9,10].

Metal structures are often subjected to low temperatures, and depending on the application, they are subject to impacts, like equipment used in mining environments when exposed to cold climates. In countries such as Russia and Canada, for example, where working temperatures can exceed $-20\text{ }^{\circ}\text{C}$, it is known, however, that ferritic materials have a ductile-brittle transition when subjected to negative temperatures [11]. The ductile-brittle transition curve is the dependence of the energy absorbed by the Charpy specimen concerning temperature [12]. Since the results obtained in the Charpy test are qualitative, obtaining the transition curve helps engineers to choose the most suitable material for applications where this loss of toughness occurs due to a drop in temperature.

Based on the increasing extent of the use of high strength steels, this work aims to assess the impact toughness in the three regions (base metal, heat-affected-zone, and weld metal) of a HARDOX 450[®] steel welded joint when subjected to temperatures below room temperature to assess the change in toughness as the temperature decreases.

2. Materials and Methods

In this article, six plates with 150 mm wide, 500 mm long, and 10 mm thick each one, were joined using the Metal Cored Arc Welding process, and it was performed manually by a welder because we did not have a mechanized or automated welding process to do this work.

A 1/2 V groove was used because this configuration facilitated the marking step to establish the specific HAZ (Figure 1) location to assist the machining of the V notch of the Charpy specimens. Using this type of groove is possible to see the fusion line in the welded joint after Nital-etched, besides the welding metal region (Figure 2).

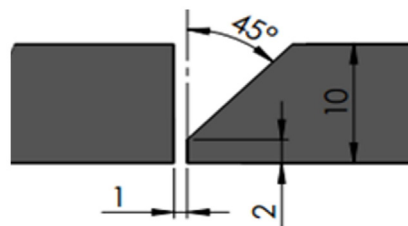


Figure 1. Joint configuration, dimensions in mm.

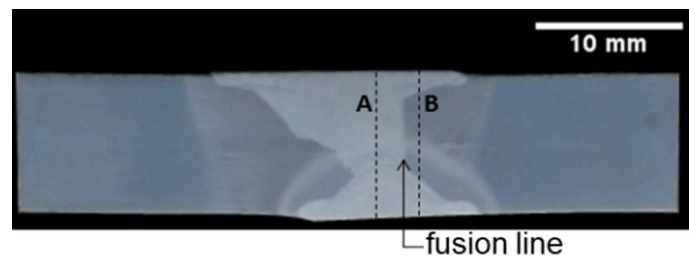


Figure 2. Macrograph illustrating the position of V-notch in the weld metal (A) and HAZ (B).

The plates were $150\text{ }^{\circ}\text{C}$ preheated with the aid of a blowtorch because its high carbon equivalent, according to the Graville diagram [13], that establishes that the material is weldable nevertheless susceptible to cold cracking. The welding procedure was carried out using two passes (a root pass and a filling pass), with the following flow rate: a mixture of Ar + 15% CO_2 (flow rate of 15 l/min) as gas protection, the direct current positive polarity of 300 A, voltage of 32 V and welding speed of approximately 0.5 m/min. These parameters resulted in a heat input of 1.04 kJ/mm.

The welded joints were analyzed using the as-welded condition with dimensions consisting of 300 mm x 500 mm x 100 mm.

A metal cored electrode ASME SFA-5.28 E110C-G with a diameter of 1.2 mm was used to carry out the welding process. Table 1 shows the chemical composition of the base metal and the electrode used the equivalent carbon of the plate.

Table 1. Base metal (Hardox 450[®]) and electrode chemical composition used.

Element	C	Si	Mn	P	S	Cr	Ni	Mo	B	Ceq*
HARDOX 450 [®]	0.165	0.214	1.30	0.0087	0.0029	0.132	0.0638	0.0207	0.0012	0.42
Tubular Wire	0.04	0.37	1.30	-	-	-	1.99	0.48	-	-

*Ceq = $\%C + (\%Mn)/6 + (\%Cr + \%Mo + \%V)/5 + (\%Cu + \%Ni)/15$

Samples were extracted from the welded material to carry out Charpy-V notch impact tests on the base metal (BM, 24 samples), weld metal (WM, 24 samples), and heat-affected zone (HAZ, 24 samples). Besides, samples to perform a tensile test on the base metal and in the region of the welded joint were taken. Figure 3 shows a schematic arrangement of the specimens on the plate. However, the figure does not represent the real number of samples in each welded plate.

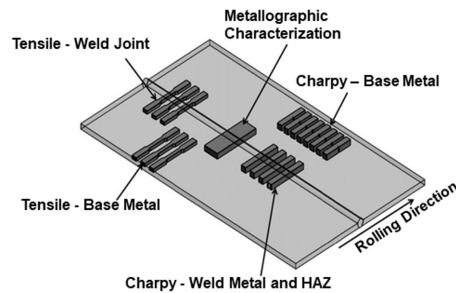


Figure 3. Schematic arrangement of samples taken on the welded plate.

The samples referring to the welded region were prepared for metallography (ground, polished, and etched with Nital 5%) to reveal the WM and the HAZ. Thus, it was possible to correctly adjust the machining position of the notch in the Charpy-V test or to position this region revealed precisely in the center of the sample for machining the specimen for the tensile test. The machining of the specimens was performed using wire electrical discharge machining. The marking for machining the V-notch in the HAZ was 1.0 mm from the fusion line (Figure 2). The samples for the Charpy impact test had the dimensions of 10 mm x 10 mm x 55 mm, according to the ASTM E23 standard [14].

A sample of the welded plate was extracted for microstructure analysis of the transverse region of the weld bead. The sample was prepared according to the following granulometric sandpaper order: 120, 220, 320, 400, 600, and 1200 mesh. Subsequently, felt polishing was performed with a diamond paste of 4.0 μm and 1.0 μm granulometry. The microstructure was revealed with Nital 2% and etched by immersion for 5 s. The sample was analyzed through a Leica optical microscope model DM2700M to identify the base metal's microstructures, the weld metal, and the heat-affected zone.

The tensile tests were performed to characterize the mechanical properties of the base metal and the welded joint; 10 tests were performed, 5 samples referring to the base metal, and 5 samples from the welded region. The tests were conducted with a temperature of 25 $^{\circ}\text{C}$, using an electromechanical machine Instron 5585 H and a loading rate of 0.45 mm/min. Sub-size specimens were used (Figure 4) according to the ASTM E8/E8M standard [15] to perform the tensile tests. The choice of this type of specimen, of smaller dimensions, is related to the high strength of the base metal because, if a standard specimen were used, the load required to break the sample would exceed the machine's capacity, which is 250 kN.

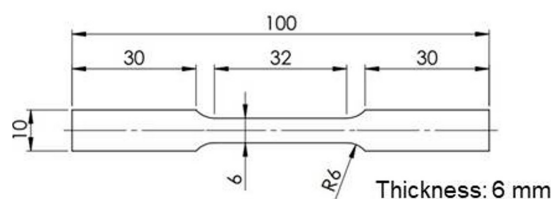


Figure 4. Tensile sample dimensions in mm of the sub-size specimen used for the base metal and welded joint.

The Charpy-V impact tests were conducted at six different temperatures (25 $^{\circ}\text{C}$, 0 $^{\circ}\text{C}$, -20 $^{\circ}\text{C}$, -60 $^{\circ}\text{C}$, -80 $^{\circ}\text{C}$, and -100 $^{\circ}\text{C}$) to obtain the ductile-brittle transition curve of the base metal (BM), weld metal (WM), and heat-affected zone (HAZ). Four (4) tests will be performed per temperature per location. The total will be 72 tests, 24 in the BM, 24 in the HAZ, and 24 in the WM.

The samples tested at low temperature undertook different procedures to obtain the desired temperature. The samples tested at 0 $^{\circ}\text{C}$ were immersed in a mixture of ethyl alcohol and ice. However, the specimens tested at temperatures of -80 $^{\circ}\text{C}$, -60 $^{\circ}\text{C}$ and -20 $^{\circ}\text{C}$ were immersed in a mixture of dry ice and ethyl alcohol. Also, the temperature of -100 $^{\circ}\text{C}$ was reached using liquid nitrogen. The temperature monitoring was performed employing a T-type thermocouple using Spider data acquisition equipment, which uses the Catman software. All samples tested at low temperature were placed in a tank specially developed for this type of procedure, where they were immersed in their respective mixtures. The soaking time of the samples at the respective temperatures and the test procedure were according to the

ASTM E-23 standard [14]. All tests were carried out on an Instron Charpy / Izod impact tester model SI-1D3 with a capacity of 400 J and impactor speed of 5.19 m/s.

3. Results and Discussion

3.1 Microstructural analysis

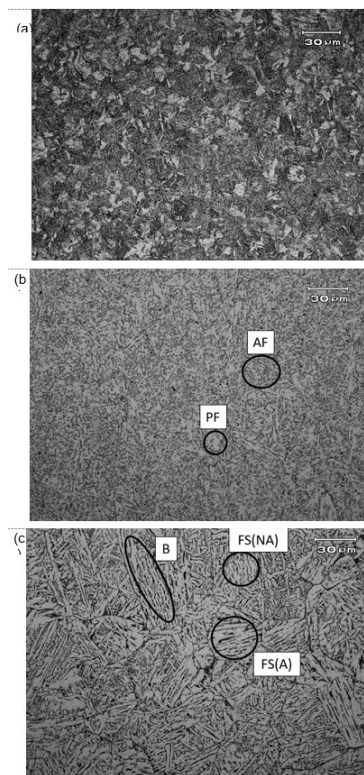


Figure 5. (a) and (b) show the microstructure of the base metal and the weld metal, respectively. (c) shows the microstructure found in the HAZ region where the marking was performed for machining notch.

Figure 5(a) Microstructure of the base metal (BM) consisting of tempered martensite, (b) microstructure of weld metal (WM) consisting of acicular ferrite (AF) and polygonal ferrite (PF) and (c) Microstructure of heat-affected-zone (HAZ) consisting of bainite (B), Widmanstätten ferrite with non-aligned second phase FS(NA), and Widmanstätten ferrite with aligned second phase FS(A).

Figure 5(a) shows a microstructure composed by tempered martensite, and it can be almost as resistant as martensite, but with increased ductility and toughness [16,17]. The microstructure of the weld metal, Figure 5(b), is predominantly composed of acicular ferrite (FA). However, it also presents polygonal ferrite (PF). A microstructure composed of acicular ferrite (AF) in the weld metal is of great importance for promoting a tough and resistant structure, and its thin and interlaced microstructure significantly prevents the initiation and propagation of cracks [16,18-20]. Concerning the microstructure found in the HAZ region, Figure 5(c), it was found a coarse grain due to the heat input of the welding process. According to the work done by Thewlis [21], the microstructure of the HAZ region is characterized by presenting bainite (B) and Widmanstätten ferrite that can be subdivided into Widmanstätten ferrite with aligned second phase FS(A) and ferrite with non-aligned second phase FS(NA). According to Eroğlu et al. [16], Widmanstätten ferrite is not desired due to its low toughness.

3.2 Mechanical tests

Table 2 shows the average values for tensile testing of the base metal and the tests related to the welded joint.

Table 2. Mechanical properties of base metal and welded joint.

Material	Yield Strength (MPa)	Tensile Strength (MPa)	Elongation (%)
BASE METAL	1167	1448	18
WELDED JOINT	523	680	15

The results obtained for the base metal are per the values provided by the manufacturer (SSAB company). However, the welded joint presented results well below those obtained with MB. This result was already expected due to a drop in mechanical resistance in the HAZ region caused by the thermal cycle of welding, which promotes an effect called soft zone. Therefore, the welded region represents a weak bond which decreases the mechanical properties obtained in the tensile test in this region [22-24].

Figure 6 shows the results of impact toughness obtained in the Charpy test in different regions (BM, WM, and HAZ). Between the temperatures of $-60\text{ }^{\circ}\text{C}$ to $25\text{ }^{\circ}\text{C}$, the toughness reduction of the weld metal to the base metal ranged from 19.5% to 23%. However, the difference in the toughness drop of the heat-affected zone compared to the base metal was greater than 32%. The datasheet from the steel supplier informed typical impact energy of 50 J tested at $-40\text{ }^{\circ}\text{C}$.

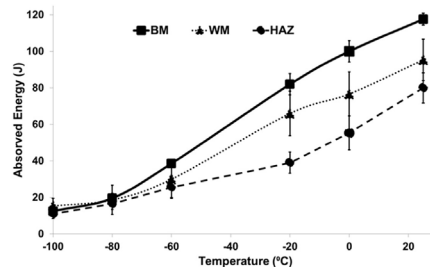


Figure 6. Ductile-brittle transition curve for base metal (BM), weld metal (WM), and heat-affected-zone regions obtained in the impact test.

Figure 7 shows some fractured specimens after the impact test where a reduction in lateral contraction can be seen with the decrease in temperature for all regions analyzed, being this fact more pronounced when comparing the samples with the temperature of $25\text{ }^{\circ}\text{C}$ with the of $-100\text{ }^{\circ}\text{C}$.

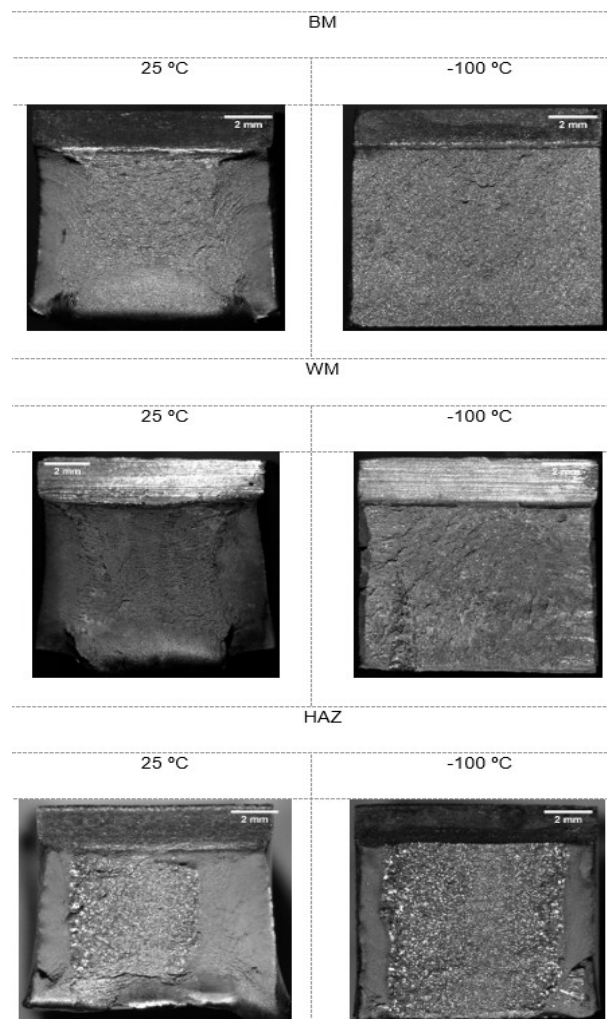


Figure 7. Fractured specimens after the Charpy-V impact test in BM, WM, and HAZ regions for temperatures of $25\text{ }^{\circ}\text{C}$ and $-100\text{ }^{\circ}\text{C}$.

The results presented in Figure 6 clearly show the influence of temperature on the value of absorbed energy in each of the tested regions. However, in addition to the decrease in temperature, the transition temperature of steels is affected by the steel cleanliness (i.e. number of inclusions per volume) and effective grain size, which are varied with the type, size, and volume fraction of phases [11].

In the study carried out by Jang et al. [12], it has been seen that the energy absorbed during the impact test depends on the stress field in front of the notch, which is directly connected to the notch position in the welded joint regions (BM, WM, and HAZ), due to the microstructural difference of each region (Figure 5), providing different mechanical properties. The relationship between the results of the BM Charpy test and its respective microstructure (tempered martensite), as well as its performance, may be associated with the addition of alloying elements like Mn, Ni, Cr, and B (Table 1) and the process of manufacturing the plate, which provides a refined microstructure, contributing to increased toughness and also mechanical resistance [4,6,17].

About WM, the presence of polygonal ferrite contributes to the decreased toughness, although the presence of acicular ferrite increases [8]. The low toughness presented in HAZ is related to its microstructure composed of Widmanstätten ferrite and coarse grain. The Widmanstätten ferrite has a structure that has parallel plates in the matrix, so it can be a path of easy crack propagation, decreasing the toughness of the material [8].

It is noticed that from the temperature of $-80\text{ }^{\circ}\text{C}$, both regions (BM, WM, and HAZ) begin to enter the lower-level region of the transition curve (Figure 6) Tests at temperatures above $25\text{ }^{\circ}\text{C}$ would have to be performed to determine the upper level of the transition curve.

4. Conclusion

According to the results obtained in the present research, the main conclusions are:

- The base metal presented superior impact toughness, and the HAZ region exhibited a worse performance due to the presence of Widmanstätten ferrite and coarse grain;
- All regions had their toughness significantly influenced by the temperature drop from $25\text{ }^{\circ}\text{C}$ to $-80\text{ }^{\circ}\text{C}$. However, from temperatures of $-80\text{ }^{\circ}\text{C}$ and $-100\text{ }^{\circ}\text{C}$, the impact energy in the three regions (BM, WM, and HAZ) showed to be similar;
- Hardox 450[®] steel welded presented satisfactory toughness conditions at low temperatures in the BM and WM regions up to a temperature of $-40\text{ }^{\circ}\text{C}$ considering the welding parameters used;
- The Heat Affected Zone had its mechanical properties compromised due to the applied welding parameters requiring attention when these joints are subjected to loads.

Authors' contributions

VMC and PHCPC: conceptualization. VMC: methodology. PHCPC: software. PHCPC: validation. VMC: resources. VMC: investigation. VMC: data curation. PHCPC and ERV: writing - original draft. PHCPC and ERV: writing - review & editing. PHCPC: visualization. PHCPC: supervision. PHCPC and ERV: project administration.

Acknowledgements

The authors would like to thank the Physical Metallurgy Laboratory-UFRGS (LAMEF), in particular Professor Telmo Strohaecker (*in memoriam*), for the possibility of carrying out and guiding this work. We would also like to thank the company Randon Implementos for donating the material used.

References

- [1] Gu L, Wang Z, Zhang Y, Guo A, Stalheim D. Development and application of the high-strength wear-resistance steel used for the lightweight, heavy-duty dump mining truck. In: HSLA Steels 2015, Microalloying 2015 & Offshore Engineering Steels 2015: Conference Proceedings. Cham: Springer; 2015. p. 549-556. <http://dx.doi.org/10.1002/9781119223399.ch66>.
- [2] Konat Ł. Structural aspects of execution and thermal treatment of welded joints of hardox extreme steel. *Metals*. 2019;9(9):915. <http://dx.doi.org/10.3390/met9090915>.
- [3] Konat Ł, Białobrzaska B, Białek P. Effect of welding process on microstructural and mechanical characteristics of Hardox 600 steel. *Metals*. 2017;7(9):349. <http://dx.doi.org/10.3390/met7090349>.
- [4] Stalheim DG, Peimao F, Linhao G, Yongqing Z. Metallurgical/alloy optimization of high strength and wear resistant structural quench and tempered steels. In: HSLA Steels 2015, Microalloying 2015 & Offshore Engineering Steels 2015: Conference Proceedings. Cham: Springer; 2015. p. 995-1001 <http://dx.doi.org/10.1002/9781119223399.ch125>.
- [5] Frydman S, Konat Ł, Pękalski G. Structure and hardness changes in welded joints of Hardox steels. *Archives of Civil and Mechanical Engineering*. 2008;8(4):15-27. [http://dx.doi.org/10.1016/S1644-9665\(12\)60118-6](http://dx.doi.org/10.1016/S1644-9665(12)60118-6).

- [6] Jun HJ, Kang JS, Seo DH, Kang KB, Park CG. Effects of deformation and boron on microstructure and continuous cooling transformation in low carbon HSLA steels. *Materials Science and Engineering A*. 2006;422(1-2):157-162. <http://dx.doi.org/10.1016/j.msea.2005.05.008>.
- [7] Kim S, Kang Y, Lee C. Variation in microstructures and mechanical properties in the coarse-grained heat-affected zone of low-alloy steel with boron content. *Materials Science and Engineering A*. 2013;559:178-186. <http://dx.doi.org/10.1016/j.msea.2012.08.072>.
- [8] Magudeeswaran G, Balasubramanian V, Madhusudhan Reddy G, Balasubramanian TS. Effect of welding processes and consumables on tensile and impact properties of high strength quenched and tempered steel joints. *Journal of Iron and Steel Research International*. 2008;15(6):87-94. [http://dx.doi.org/10.1016/S1006-706X\(08\)60273-3](http://dx.doi.org/10.1016/S1006-706X(08)60273-3).
- [9] Mohamat SA, Ibrahim IA, Amir A, Ghalib A. The effect of Flux Core Arc Welding (FCAW) processes on different parameters. *Procedia Engineering*. 2012;41:1497-1501. <http://dx.doi.org/10.1016/j.proeng.2012.07.341>.
- [10] Starling CMD, Modenesi PJ, Borba TMD. Caracterização do cordão na soldagem FCAW com um arame tubular "Metal cored.". *Soldagem e Inspeção*. 2011;16(3):285-300. <http://dx.doi.org/10.1590/S0104-92242011000300010>.
- [11] Shin SY, Hwang B, Lee S, Kim NJ, Ahn SS. Correlation of microstructure and Charpy impact properties in API X70 and X80 line-pipe steels. *Materials Science and Engineering A*. 2007;458(1-2):281-289. <http://dx.doi.org/10.1016/j.msea.2006.12.097>.
- [12] Jang YC, Hong JK, Park JH, Kim DW, Lee Y. Effects of notch position of the Charpy impact specimen on the failure behavior in the heat-affected zone. *Journal of Materials Processing Technology*. 2008;201(1-3):419-424. <http://dx.doi.org/10.1016/j.jmatprotec.2007.11.272>.
- [13] Datta R, Mukerjee D, Jha S, Narasimhan K, Veeraraghavan R. Weldability characteristics of shielded metal arc welded high strength quenched and tempered plates. *Journal of Materials Engineering and Performance*. 2002;11(1):5-10. <http://dx.doi.org/10.1007/s11665-002-0001-7>.
- [14] American Society for Testing and Materials. ASTM E23-12c: standard test methods for notched bar impact testing of metallic materials. West Conshohocken: ASTM; 2013.
- [15] American Society for Testing and Materials. ASTM E8/E8M: standard test methods for tension testing of metallic materials. West Conshohocken: ASTM; 2010.
- [16] Eroğlu M, Aksoy M, Orhan N. Effect of coarse initial grain size on microstructure and mechanical properties of weld metal and HAZ of a low carbon steel. *Materials Science and Engineering A*. 1999;269(1-2):59-66. [http://dx.doi.org/10.1016/S0921-5093\(99\)00137-9](http://dx.doi.org/10.1016/S0921-5093(99)00137-9).
- [17] Krauss G. Deformation and fracture in martensitic carbon steels tempered at low temperatures. *Metallurgical and Materials Transactions. B, Process Metallurgy and Materials Processing Science*. 2001;32(2):205-221. <http://dx.doi.org/10.1007/s11663-001-0044-4>.
- [18] Fattahi M, Nabhani N, Hosseini M, Arabian N, Rahimi E. Effect of Ti-containing inclusions on the nucleation of acicular ferrite and mechanical properties of multipass weld metals. *Micron (Oxford, England)*. 2013;45:107-114. <http://dx.doi.org/10.1016/j.micron.2012.11.004>. PMID:23238108.
- [19] Babu SS. The mechanism of acicular ferrite in weld deposits. *Current Opinion in Solid State and Materials Science*. 2004;8(3-4):267-278. <http://dx.doi.org/10.1016/j.cossms.2004.10.001>.
- [20] Xiong Z, Liu S, Wang X, Shang C, Li X, Misra RDK. The contribution of intragranular acicular ferrite microstructural constituent on impact toughness and impeding crack initiation and propagation in the heat-affected zone (HAZ) of low-carbon steels. *Materials Science and Engineering A*. 2015;636:117-123. <http://dx.doi.org/10.1016/j.msea.2015.03.090>.
- [21] Thewlis G. Materials perspective: classification and quantification of microstructures in steels. *Materials Science and Technology*. 2004;20(2):143-160. <http://dx.doi.org/10.1179/026708304225010325>.
- [22] Sharma V, Shahi AS. Effect of groove design on mechanical and metallurgical properties of quenched and tempered low alloy abrasion resistant steel welded joints. *Materials & Design*. 2014;53:727-736. <http://dx.doi.org/10.1016/j.matdes.2013.07.043>.
- [23] Ryabov VV, Kniaziuk TV, Mikhailov MS, Motovilina GD, Khlusova EI. Structure and properties of new wear-resistant steels for agricultural machine building. *Inorganic Materials: Applied Research*. 2017;8(6):827-836. <http://dx.doi.org/10.1134/S2075113317060120>.
- [24] Mohandas T, Madhusudan Reddy G, Satish Kumar B. Heat-affected zone softening in high-strength low-alloy steels. *Journal of Materials Processing Technology*. 1999;88(1):284-294. [http://dx.doi.org/10.1016/S0924-0136\(98\)00404-X](http://dx.doi.org/10.1016/S0924-0136(98)00404-X).